20

Zeolitic Imidazolate Frameworks

20.1 Introduction

Zeolitic imidazolate frameworks (ZIFs) are a subclass of metal-organic frameworks (MOFs). Similar to MOFs, their structures are built from organic linkers and inorganic nodes. However, whereas MOF structures typically consist of linkers bearing chelating functionalities (e.g. carboxylate, pyrazolate) favoring the formation of polynuclear secondary building units (SBUs), the imidazole linkers used to construct ZIFs induce the formation of tetrahedral single transition metal nodes, and therefore the formation of tetrahedral topologies as in zeolites is favored (Figure 20.1). The strong interaction between the charged imidazolate linkers and the metal ions, in combination with the preference for the formation of rigid cages, renders ZIFs highly robust porous materials, thus setting them apart from classic coordination networks (see Chapter 1). As the name suggests, the structures of ZIFs are closely related to those of zeolites, which is ascribed to the combination of tetrahedral nodes and bent linkers mimicking the structural features of zeolites. In ZIFs, the angle between two metal centers bridged by an imidazolate unit is typically ∠(M–imidazolate–M) = 145°, a value close or even identical to that found for the ∠(Si–O–Si) angle in zeolites. To understand the development of porous metal-organic materials with zeolitic structures it is instructive to discuss the development of zeolites and their underlying structural chemistry.

The name zeolite is derived from the Greek ζέω (*zéō*), meaning "to boil" and λίθος (*líthos*), meaning "stone." Zeolites are crystalline aluminosilicates of group I and II elements (Na, K, Mg, Ca) with the general chemical formula $M_{2/n}O \cdot Al_2O_3 \cdot ySiO_2 \cdot wH_2O$, where n is the cation valence, y is 2–200, and w is the amount of water contained in the pores. They can be described as complex crystalline purely inorganic extended structures. The primary structural units (AlO_4 or SiO_4) are linked into larger so-called secondary building units that are linked to form extended 3D framework structures with pore sizes typically ranging from 0.3 to 1.0 nm and pore volumes between 0.10 and 0.35 $cm^3\ g^{-1}$. The presence of AlO_4 units in the silicate structures leads to charged cationic frameworks with counter ions residing within their pores. The term "zeolite" was coined by the Swedish mineralogist Alex F. Cronstedt in 1756 who discovered the first zeolite mineral (Stilbite) and observed that the material liberated large

Introduction to Reticular Chemistry: Metal-Organic Frameworks and Covalent Organic Frameworks,
First Edition. Omar M. Yaghi, Markus J. Kalmutzki, and Christian S. Diercks.

Companion website: www.wiley.com/go/yaghi/reticular

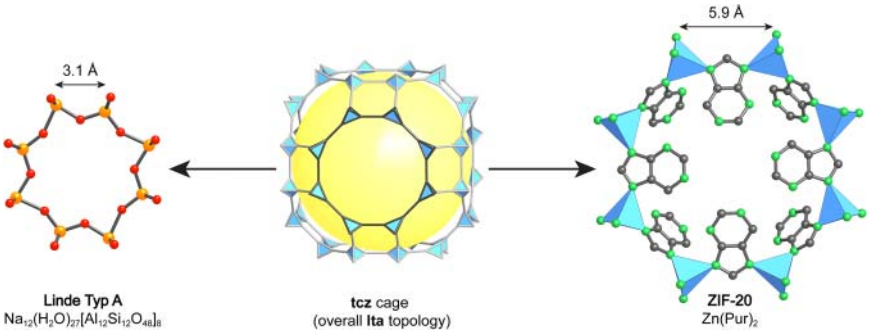

Figure 20.1 Zeolite versus ZIF: comparison of the 8-membered rings constituting the **tcz** cages in frameworks of **lta** topology. The silicon/aluminum nodes of the zeolite structure are replaced by tetrahedral metal ions (here Zn) and the oxygen links are replaced by imidazole-based linkers (here Pur = purine). Color code: Zn, blue; C, gray; N, green; O, red; Al and Si, orange.

quantities of "steam" when heated [1]. In 1840 Augustin A. Damour reported that zeolites are indeed capable of reversible uptake of water with no apparent change in morphology [2]. Twenty-two years later Henri É. Saint Claire-Deville described the first hydrothermal synthesis of a zeolite: levynite, a naturally occurring mineral [3]. At this point, only little was known about the properties of zeolites and it was not until 1896 that Georges Friedel developed the idea that the structure of dehydrated zeolites is similar to an open sponge-like framework, after having observed the occlusion of various liquids such as alcohol, benzene, and chloroform by dehydrated zeolites [4]. In the mid-1930s Richard M. Barrer began his pioneering work on zeolites, studying their synthesis and adsorption properties, in particular the diffusion of ions in open structures and subsequently classified them according to their pore sizes [5]. In 1948, Barrer reported the first definitive synthesis of zeolites, including both a synthetic analog of a zeolite mineral (Mordenite) and a novel, synthetic zeolite (KFI) [6]. With a steadily increasing number of synthetically accessible zeolites and a growing interest in their properties, their properties were studied in the search for new approaches to the separation and purification of air. In the mid- to late-1940s, Robert M. Milton confirmed that zeolites are indeed capable of reversible gas adsorption, rendering them highly interesting materials for industrial applications. The 1980s was a period of discovery of new zeolites. Extensive work on the synthesis and applications of ZSM-5 ($Na_nAl_nSi_{96-n}O_{192}\cdot 16H_2O$, where $0 < n < 27$) and a growing number of other members of the high silica zeolite family led to the discovery of microporous crystalline aluminophosphate molecular sieves in 1982 by Stephen T. Wilson et al. at Union Carbide [7]. Soon after, many more members of the family of aluminophosphates, SAPO, MeAPO, MeAPSO, ElAPO, and ElAPSO, were discovered and efforts to synthesize metallosilicate molecular sieves containing elements other than silicon and aluminum, such as titanium, iron, gallium, or germanium, were made [8]. Until today, the combination of different tetrahedral MO_4 units linked to form larger 3D entities gave rise to about 180 different structure types [9]. The definite geometry of the tetrahedral

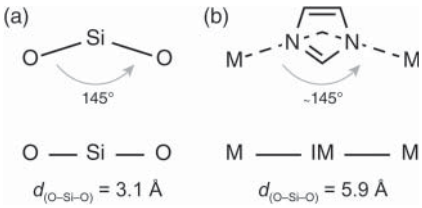

Figure 20.2 (a) Comparison of ∠(O–Si–O) in zeolites and (b) the ∠(M–IM–M) angle in ZIFs. Both are approximately 145°, but the O–Si–O-distance is 3.1 Å compared to the M–IM–M distance of 5.9 Å, leading to expanded pore sizes for identical topologies in ZIFs.

building units provides zeolites with rigid architecturally and mechanically stable structures. Even though a wide variety of different structures is accessible and certain methods for their functionalization have been established, zeolites suffer from the inherent limitation imparted by their inorganic building units. In a manner akin to that described for carboxylate MOFs, extended metal-organic materials with zeolitic structures can be prepared by judicious choice of appropriate starting materials. In order to prepare extended framework structures with tetrahedral (zeolitic) topologies, tetrahedral nodes have to be linked by building units with an angle close to, if not identical to, that of the ∠(Si–O–Si) = 145° fragment found in zeolites [10]. With an average ∠(M–imidazolate–M) angle of around 145°, imidazoles satisfy this prerequisite (Figure 20.2).[1]

Their reticulation with metal ions leads to the formation of structures with tetrahedrally coordinated metal cations playing the role of the tetrahedral silicon/aluminum atoms and the imidazolate anions forming bridges that mimic the role of oxygen atoms in zeolites [11]. Today, ZIFs with more than 100 different topologies, often analogous, but not limited to those known in zeolite chemistry, have been synthesized and structurally characterized. Their open permanently porous structures initiated intense research in the field of ZIFs, mostly driven by the prospect of expanding their pore sizes, functionalizing their pores, and exploring new sorption, separation, and catalytic properties [10c, 11].

20.2 Zeolitic Framework Structures

Extended metal-organic materials with zeolitic structures are divided into two groups: ZIFs and Z-MOFs. In analogy to MOFs, the topologies of Z-MOFs are commonly referred to by a lower case (bold) three-letter code (e.g. **rho**, the codes are identical to the RCSR codes) whereas zeolites and ZIFs having zeolite topologies are often given an uppercase three-letter code (e.g. RHO, as implemented by the Structure Commission of the International Zeolite Association, "IZA"). Throughout this chapter all topologies will be referred to with their three-letter codes according to the RCSR.

20.2.1 Zeolite-Like Metal-Organic Frameworks (Z-MOFs)

Z-MOFs are typically constructed from carboxylate functionalized imidazoles or pyrimidine units and tetrahedrally coordinated single-metal nodes linked together into tetrahedral structures. In contrast to the formation reactions of

1 Some MOFs fulfill these requirements as well and form tetrahedral structures. Owing to this they are commonly referred to as Z-MOFs. For more details, the reader is referred elsewhere [10a].

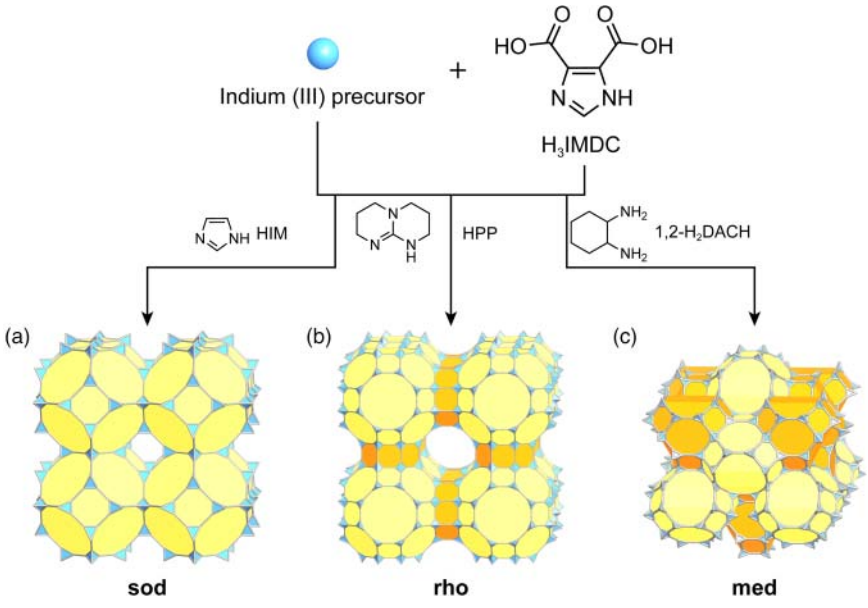

Figure 20.3 Synthesis of Z-MOFs by reticulating indium ions and H_3IMDC (imidazole dicarboxylic acid) in the presence of different SDAs. Three different framework topologies are realized. (a) A framework of **sod** topology forms in the presence of HIM, (b) the **rho** topology is favored in the presence of HHP, (c) and a framework of **med** topology is obtained when 1,2-H_2DACH is used [13].

MOFs based on polynuclear SBUs, the formation of Z-MOFs often requires the presence of a structure-directing agent (SDA) and a mixture of the same components can result in different topologies depending on the SDA used. Reticulation of In^{3+} ions and H_3IMDC (1*H*-imidazole-4,5-dicarboxylic acid) with three different SDAs yields three Z-MOFs of different topologies [12]. The presence of imidazole (HIM) affords the formation of a Z-MOF with **sod** topology (Figure 20.3a), HPP (1,3,4,6,7,8-hexahydro-2*H*-pyrimido[1,2-*a*]pyrimidine) affords the formation of an **rho** topology (Figure 20.3b), and the presence of 1,2-H_2DACH (1,2-diaminocyclohexane) affords the formation of an **med** net (Figure 20.3c), a topology not known for zeolites. In the **sod** Z-MOF, each indium center is 6-coordinate by two hetero-chelating HIMDC linkers and two HIMDC nitrogen donors, leading to the desired tetrahedral $InN_4(–COO)_2$ building unit. In contrast, in the **rho** Z-MOF each indium center is 8-coordinate by four hetero-chelating HIMDC linkers to give tetrahedral $InN_4(–COO)_4$ building units. Both materials possess pore volumes that are up to eight times as large than those of their purely inorganic counterparts. In the structure of **usf**-Z-MOF (**med** topology), the indium single-metal nodes are coordinated in a tetrahedral manner by four HIMDC linkers forming 8-c $InN_4(COO)_4$ building units [13]. A comparison of all three topologies is given in Figure 20.3.

Since, in terms of topology, the vertices and nodes can be chosen in such way that a significant simplification of the overall structure is achieved, tetrahedral

subunits assembled from SBUs and carboxylate linkers can also be described by tetrahedral, zeolite-like topologies [10a, 14]. We already encountered such MOFs with zeolite-like structures in earlier chapters exemplified by MIL-100 and MIL-101, both of which are built from vertex-sharing tetrahedral tertiary building units (TBUs) resulting in an overall tetrahedral **mtn** topology (see Figure 2.13) [14].

20.2.2 Zeolitic Imidazolate Frameworks (ZIFs)

As outlined earlier, imidazolates can link tetrahedral metal centers with an M–IM–M angle close to 145°, which is not the case for triazolates or tetrazolates, making imidazolates ideal building units for extended structures with tetrahedral, zeolite-like topologies. The combination of imidazole derivatives and tetrahedral metal nodes allows for the formation of a wide range of different ZIF structures. The strong bond between the charged imidazolate linker and the metal center along with the hydrophobic nature of ZIFs gives rise to high chemical and thermal stability, whereas their tetrahedral structures provide for high mechanical and architectural stability. These properties, in combination with the chemical tunability inherent to reticular materials, make ZIFs interesting in the context of gas adsorption, gas separation, and catalysis.

Early examples of ZIFs were limited to non-porous, dense structures. This can be ascribed to the fact that the energetically most favorable spatial arrangement for the combination of tetrahedral metal nodes and (unsubstituted) imidazolate units is also the most dense one [15]. The development of porous ZIFs featuring characteristics of both zeolites and MOFs, combining uniform cage-like pores with high crystallinity and permanent porosity, initiated intense research in this field. In contrast to the pores without walls commonly observed in carboxylate-based MOFs (see Chapters 1–6), the structures of ZIFs are typically built form cages composed of multiple fused rings of metal nodes connected by imidazolate linkers. Therefore, the pore opening is dictated by the size of the rings constituting these cages and is thus often relatively small. The specific architecture of these cages in combination with the relatively short imidazole linker endow ZIFs with mechanical and architectural stability and allows them to support permanent porosity. Indeed, ZIFs are often more stable than other extended metal-organic materials as highlighted by the fact that ZIF-8 retains both crystallinity and porosity when refluxed in water, alkaline solutions, or organic solvents over an extended period of time.

The functionalization of the imidazole linker can be achieved in manners akin to those used to functionalize MOFs (see Chapter 6). Pre-synthetic functionalization of the imidazole linker not only imparts functionality but the steric demand of the functionality appended to the linker as well as its position also has an impact on the structure formed upon reticulation. Design principles making use of this finding allow for the design and synthesis of ZIFs built from cages of specific size and we will discuss them in more detail later in this chapter. Some examples of imidazole derivatives used in the synthesis of ZIFs are given in Figure 20.4. Before elucidating the principles underlying the design of new ZIFs, it is instructive to take a closer look at typical synthetic approaches.

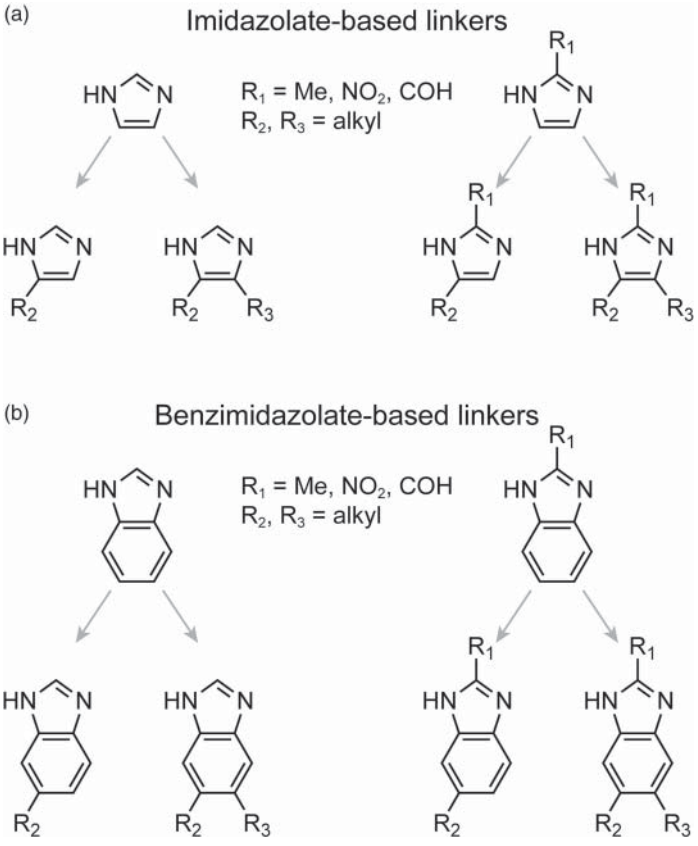

Figure 20.4 (a) Imidazolate and (b) benzimidazolate linkers used to construct ZIFs. Different substitution patterns are shown and typical substituents are given. Functionalization can be performed pre- or post-synthetically allowing for the synthesis of a wide range of structures with different functionalities.

20.3 Synthesis of ZIFs

While SDAs, such as templates, are commonly used in the synthesis of zeolites and Z-MOFs, the formation of ZIFs does not rely on such additives. ZIFs are commonly prepared by reacting the appropriate hydrated metal salts, most often zinc and other metals that prefer a tetrahedral coordination, and an imidazole (or functionalized derivatives) in an amide solution (e.g. DMF, DEF) at temperatures ranging from 85 to 150 °C. Similar to the synthesis of carboxylate-based frameworks, the slow release of amine base upon decomposition of the amide at elevated temperatures deprotonates the linker and thereby initiates framework formation. A similarly slow deprotonation is achieved by layering of solutions. This method is used to synthesize ZIF-8. Here, a solution of HmIM (2-methylimidazole) and 2,2′-bipyridine in ethanol is layered onto a solution of $[Zn(OAc)_2]\cdot 2H_2O$ dissolved in concentrated aqueous ammonia [16].

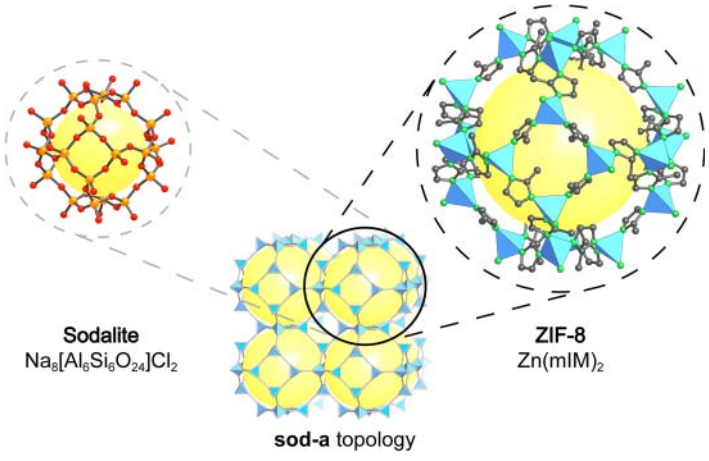

Figure 20.5 The augmented **sod** net is named after the natural mineral Sodalite. It is built from cages of **tro** topology that are connected through 4-membered rings. Each **tro** cage is built from 24 tetrahedral nodes. Owing to the increased distance of the tetrahedral nodes in ZIFs compared to zeolites, their pores are significantly larger. The **tro** cages in ZIF-8 ($Zn(mIM)_2$) have a diameter of 11.6 Å and a pore apertures of 3.4 Å. Color code: Zn, blue; C, gray; N, green; O, red; Al and Si, orange.

The slow diffusion between the layers provides for low reaction rates and thus for the reversibility required to afford a crystalline product of chemical formula $Zn(mIM)_2$, termed ZIF-8. The structure has a sodalite topology (SOD or **sod**), named after the naturally occurring mineral sodalite. The augmented **sod** net alongside the fundamental **tro** cages of sodalite and ZIF-8 are depicted in Figure 20.5. The **tro** cages in the structure of ZIF-8 have a diameter of 11.6 Å and are constructed from 4- to 6-membered rings that are fused along common edges [$4^6.6^8$]. Connecting these cages through the 4-membered rings results in a 3D pore system with channels of 3.4 Å.

The formation of frameworks with a wide range of topologies can be realized by employing substituted imidazole linkers in the synthesis. The specific substitution pattern directs the formation of different topologies and a precise design of the linker is therefore inevitable.

20.4 Prominent ZIF Structures

The structures of ZIFs are built from tetrahedral nodes that are geometrically similar to the MO_4 units in zeolites. All zeolite nets found in ZIFs are uninodal, whereas for zeolites, the majority of their nets is not. The number of possible structures built from tetrahedral units is expected to increase exponentially with the number of chemically different vertices and edges, which illustrates the vast structural possibilities of ZIF chemistry. Table 20.1 shows a compilation of frequently encountered topologies alongside representative ZIF structures. A selection of zeolite topologies found in ZIF chemistry is shown in Figure 20.6.

Table 20.1 Compilation of ZIFs, their chemical formulae, and topologies.

Common name	Chemical composition	RCSR code	Zeolite code	References
ZIF-14	$Zn(eIM)_2$	**ana**	ANA	[17]
ZIF-386	$Zn(nBIM)_{0.85}(nIM)_{0.70}(IM)_{0.45}$	—	AFX	[18]
ZIF-725	$Zn(bBIM)_{1.35}(nIM)_{0.40}(IM)_{0.25}$	**bam**	—	[18]
ZIF-62	$Co(IM)_2$	**cag**	—	[17b]
ZIF-303	$Zn(cBIM)_{0.70}(nIM)_{0.30}(IM)_{1.00}$	—	CHA	[18]
TIF-4	$Zn(IM)_{1.5}(mBIM)_{0.5}$	**coi**	—	[19]
ZIF-64	$Zn(IM)_2$	**crb**	BCT	[17b]
—	$Pr(IM)_5$	**crs**	—	[10c]
ZIF-3	$Zn_2(IM)_4$	**dft**	—	[20]
ZIF-23	$Zn(4ab\backslash BIM)_2$	**dia**	—	[21]
BIF-6	$CuBH(IM)_3$	**fes**	—	[22]
ZIF-73	$Zn(nIM)_{1.74}(mBIM)_{0.26}$	**frl**	—	[17b]
ZIF-5	$Zn_3In_2(IM)_{12}$	**gar**	—	[20]
ZIF-615	$Zn(cBIM)_{1.05}(4\text{-}nIM)_{0.95}$	**gcc**	—	[18]
ZIF-6	$Zn(IM)_2$	**gis**	GIS	[20]
ZIF-486	$Zn(nBIM)_{0.20}(mIM)_{0.65}(IM)_{1.15}$	**gme**	GME	[18]
ZIF-360	$Zn(bBIM)_{1.00}(nIM)_{0.70}(IM)_{0.30}$	**kfi**	KFI	[18]
ZIF-72	$Zn(dcIM)_2$	**lcs**	—	[17b]
ZIF-376	$Zn(nBIM)_{0.25}(mIM)_{0.25}(IM)_{1.50}$	**lta**	LTA	[18]
—	$Cd(Im)_2bipy$	**mab**	—	[23]
ZIF-60	$Zn_2(IM)_3(mIM)$	**mer**	MER	[17b]
—	$Cu(IM)_2$	**mog**	—	[24]
ZIF-100	$Zn_{20}(cBIM)_{39}(OH)$	**moz**	—	[10b]
—	$Co(IM)_2$	**neb**	—	[25]
—	$Co_2(IM)_4$	**nog**	—	[25]
TIF-3	Zn(IM)(mBIM)	**pcb**	ACO	[26]
ZIF-95	$Zn(cBIM)_2$	**poz**	—	[10b]
—	$Fe(mIM)_2$	**qtz**	—	[27]
ZIF-11	$Zn(BIM)_2$	**rho**	RHO	[20]
ZIF-8	$Zn(mIM)_2$	**sod**	SOD	[16]
BIF-8	$CuBH(eIM)_3$	**srs-c-b**	—	[22]
BIF-7	CuBH(mIM)3	**ths-c-b**	—	[22]
ZIF-412	$Zn(BIM)_{1.13}(nIM)_{0.62}(IM)_{0.25}$	**ucb**	—	[18]
ZIF-516	$Zn(mBIM)_{1.23}(bBIM)_{0.77}$	**ykh**	—	[18]
TIF-1Zn	$Zn(dmBIM)_2$	**zea**	—	[28]
TIF-2	$Zn(IM)_{1.1}(mBIM)_{0.9}$	**zeb**	—	[26]
ZIF-61	Zn(IM)(mIM)	**zni**	—	[17b]

Topologies are given both as the notation referring to zeolite topologies and those found in the RCSR database.

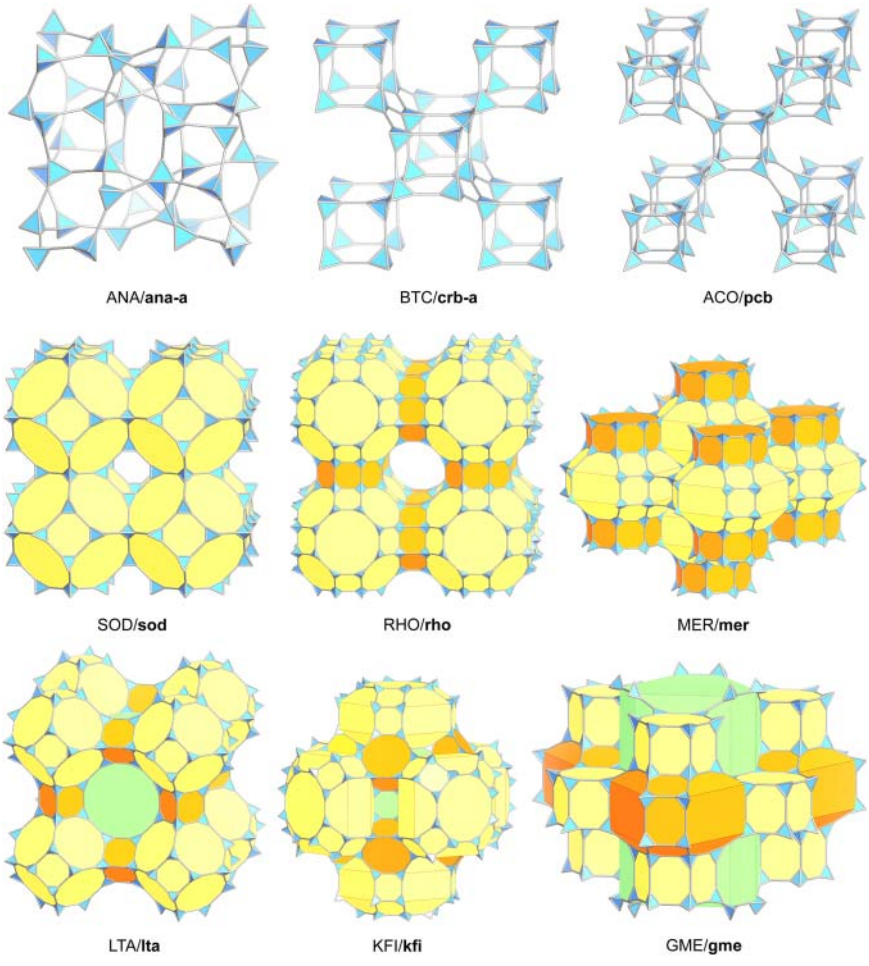

Figure 20.6 Zeolite topologies commonly found in ZIF chemistry. All frameworks are constructed from tetrahedral nodes but differ in the types of rings formed by linking these nodes. Each blue tetrahedron represents a metal node, and the differently colored polyhedra indicate different types of cage. The following frameworks are shown: ANA (**ana**), BTC (**crb**), ACO (**pcb**), SOD (**sod**), RHO (**rho**), MER (**mer**), LTA (**lta**), KFO (**kfi**), and GME (**gme**). Capitalized three-letter codes are used to describe zeolite topologies, while MOF and ZIF topologies are referred to by lowercase bolded three-letter codes.

20.5 Design of ZIFs

Even though it is known that experimental parameters such as the temperature, the concentration of starting materials, and the solvents employed can influence the formation of ZIFs in terms of topology, there are no general principles for their rationalization. In MOF chemistry, the precise geometry of the linker allows to direct the synthesis toward specific topologies. Structural consideration of the imidazole linker in general and the steric demand of its substituents in particular form the basis of the three general design principles that allow for the

rational design of ZIFs by linker-directed synthesis: (i) the maximum size of the pore opening is determined by the size and shape of the imidazole linker, which is described by a steric index (δ); (ii) the combination of linkers with large and small δ is required for the formation of large cages; and (iii) changing the ratio of a given set of imidazole linkers facilitates the formation of cages with different topologies and metrics.

20.5.1 The Steric Index δ as a Design Tool

The framework formation of ZIFs is mainly guided by the substitution pattern of the imidazole linkers employed in their synthesis. Imidazole can be substituted in two distinguishable positions: (i) the 2-position and (ii) the 4- and 5-position. We define distances in the molecular structure of the imidazole linker that are correlated to the size of appended functionalities in these positions. The size of substituents in the 2-position defines l_2 whereas substituents in the 4- or 5-positions influence the value of $l_{4,5}$ (Figure 20.7). Based on these two distances we can calculate the steric index δ according to Eq. (20.1):

$$\delta = V \times l \tag{20.1}$$

where V is the van der Waals volume of the linker and l the longer distance (l_2 or $l_{4,5}$). The steric index gives a measure of the size and shape of a given imidazole linker. Figure 20.7 gives examples of different imidazole linkers and their respective steric indices δ.

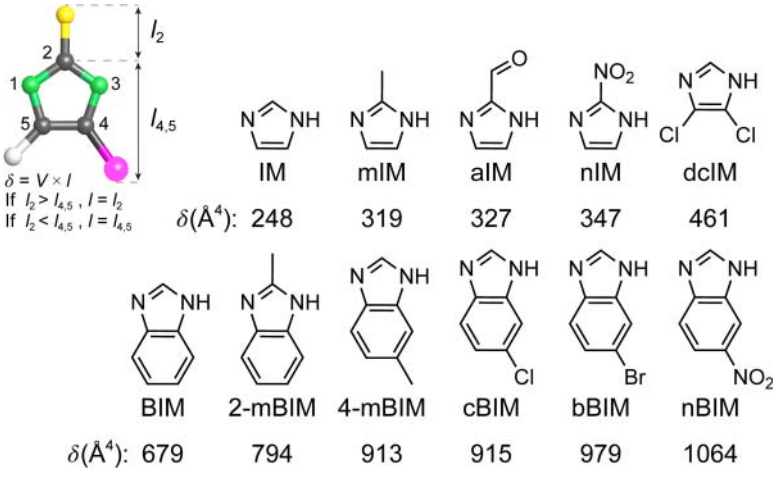

Figure 20.7 Definition of the steric index (δ). Two lengths are defined, l_2 and $l_{4,5}$. For the calculation of the steric index only the larger value is used and multiplied with the van der Waals volume of the linker. Several examples of substituted imidazoles and benzimidazoles are shown and their respective values of δ are given. Color code: N, green; C, gray; substituents in the 2-, 4-, and 5-position are shown in yellow, pink, and white, respectively.

20.5.1.1 Principle I: Control over the Maximum Pore Opening

The size of the largest ring (pore opening) in ZIFs is correlated to the steric index of the imidazole linker constituting this particular ring. To take advantage of this principle it is instructive to search for regularities in the orientation of differently substituted imidazolate linkers with respect to the ring they are forming. In general, substituents in the 2-position tend to point into the small (mostly 4-membered) rings, whereas substituents in the 4- and 5-position are pointing toward the center of 8-membered and larger rings, and both the 2- and 4-/5-positions are found to point into 6-membered rings. In structures built from cages that are constructed from fused 8-membered rings, substituents in the 4- and 5-positions are necessarily forced to point toward the center of the 4-membered rings. Thus, such structures can only form if the substituents on the 4- and 5-positions are comparatively small. This entails that increasing the bulkiness of substituents in the 4- and 5-positions, which equals a longer distance $l_{4,5}$ and therefore a large steric index δ, will inevitably lead to the formation of large rings. Since the 2-position points toward the center of the small rings due to its low steric demand, the formation of small rings is not precluded when linkers with large δ arising from large values of $l_{4,5}$ are used. The same holds true for structures built from a combination of linkers with large and small δ. In contrast, large rings cannot be obtained when only linkers with small δ are used. The first principle can be summarized as follows: the steric index δ of the imidazole linker dictates the maximum ring size and therefore the size of the pore opening of the resulting ZIF structure.

20.5.1.2 Principle II: Control over the Maximum Cage Size

The presence of large rings within a ZIF structure realized by employing imidazole linkers with large δ is not necessarily synonymous to the presence of large cages. The formation of large cages (or large internal pores) in tetrahedral structures relies on a combination of both large and small rings. Hence, to design a ZIF structure composed of large cages, it is necessary to mix both linkers with small and large δ in the appropriate ratio. The importance of balancing the ratio of imidazole linkers with large and small δ becomes clear when comparing the structures of ZIF-412 ($Zn(BIM)_{1.13}(nIM)_{0.62}(IM)_{0.25}$) and ZIF-68 (Zn(BIM)(nIM), where BIM = benzimidazolate, nIM = 2-nitroimiazolate, and IM = imidazolate) (Figure 20.8). Both structures contain 8- and 12-membered rings facilitated by sterically demanding BIM and nIM linkers with large δ of 679 and 347 Å^4, respectively. However, the largest cage in ZIF-412 is twice the size of that in ZIF-68 due to the additional comparatively small IM linker ($\delta = 248$ Å^4). This can be explained by the fact that the small IM linker enables the formation of 4- and 6-membered rings that can combine with the larger rings built from the bulkier BIM and nIM linkers to form large cages. In general, the largest cages are found in structures containing 75–90% of bulky (large δ) and 10–25% of small linkers (small δ). Thus far, ZIF-412 marks the largest cage reported for ZIFs.

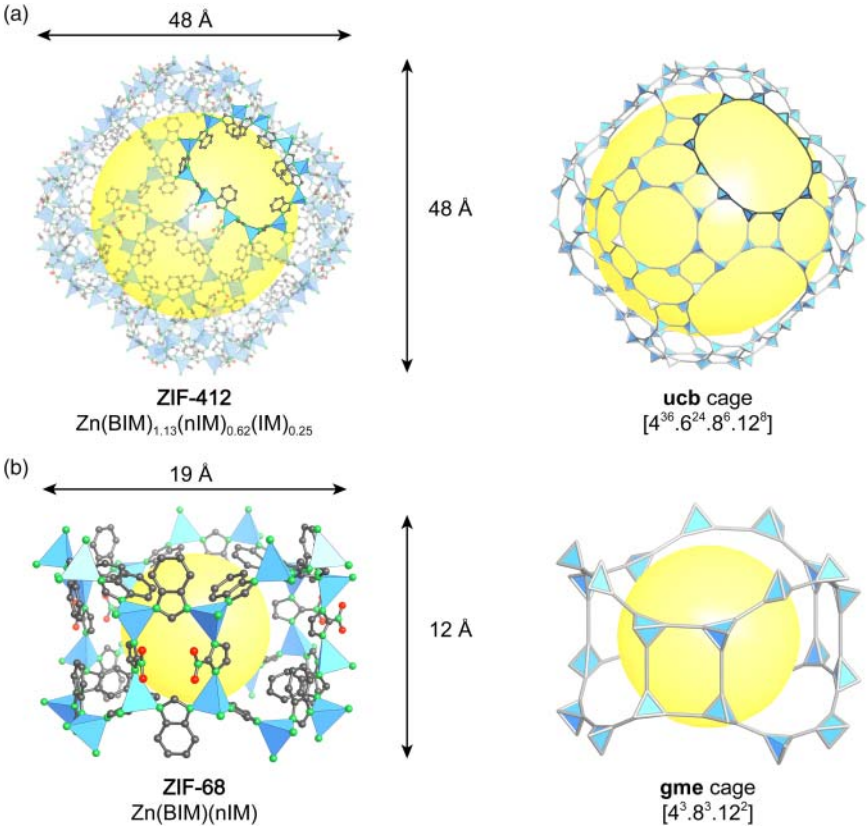

Figure 20.8 Comparison of the largest cages found in the crystal structures of ZIF-412 and ZIF-68 [17b, 18]. (a) The largest cage in ZIF-412 is built from 36 4-membered, 24 6-membered, 6 8-membered, and 8 12-membered rings and measures 48 Å in diameter. (b) The largest cage in ZIF-68 is significantly smaller due to the lack of IM linkers (small δ). It consists of only three 4-membered, three 8-membered, and two 12-membered rings. In both cases, the largest cage is shown as a crystal structure representation alongside the corresponding topology. This comparison highlights the importance of linkers with small values of δ for the formation of large cages. Color code: Zn, blue; C, gray; N, green; O, red.

20.5.1.3 Principle III: Control over the Structural Tunability

The two principles discussed above provide a rationale for the design of ZIF structures with large rings and large cages. The ratio of imidazole linkers with different steric indices provides an additional tool to access a variety of structures built from the same general components. Employing linkers with different δ therefore not only allows for the formation of structures with the maximum pore opening or cage size, but the variation of the ratio of the linkers further facilitates the formation of structures with ring and pore sizes of any value up to that maximum. The more complex the composition, meaning the larger the number

of differently substituted imidazole linkers used, the more potent this principle gets, providing access to an almost infinite number of structures. This can be illustrated by the finding that three ZIFs with different underlying topologies are formed when Zn^{2+} ions are reticulated with a mixture of different ratios of nbIM ($\delta = 1064\,Å^4$), mIM ($\delta = 319\,Å^4$), and IM linkers ($\delta = 248\,Å^4$); ZIF-486 ($Zn(nbIM)_{0.20}(mIM)_{0.65}(IM)_{1.15}$, **gme**), ZIF-376 ($Zn(nbIM)_{0.25}(mIM)_{0.25}(IM)_{1.5}$, **lta**), and ZIF-414 ($Zn(nbIM)_{0.91}(mIM)_{0.62}(IM)_{0.47}$, **ucb**). The largest cages in the structures vary between 22.6, 27.5, and 45.8 Å, respectively.

20.5.2 Functionalization of ZIFs

Applying methods similar or identical to those described in Chapter 6, ZIFs can be functionalized pre-synthetically, *in situ*, or by post-synthetic modification (PSM) – a broadness of possible functionalization not known for their inorganic zeolite counterparts. Here, we will discuss a few selected examples of the functionalization and modification of ZIFs.

To introduce functionality by performing reactions on the organic backbone of a ZIF, functional groups facilitating these reactions must be installed pre-synthetically or by linker exchange. An imidazole linker that carries a suitable functional group is aIM (1*H*-imidazole-2-carbaldehyde). The aldehyde group in the 2-posititon can be reacted with amines to form an imine bond or it can be reduced to give an alcohol group using reducing agents such as $NaBH_4$. The reaction of ZIF-90 ($Zn(aIM)_2$), a framework of **sod** topology built from aIM linkers and Zn^{2+} nodes, with ethanolamine yields ZIF-92 and reduction of ZIF-90 with $NaBH_4$ yields ZIF-91 (Figure 20.9) [29]. In both cases the crystallinity and porosity of the framework is retained.

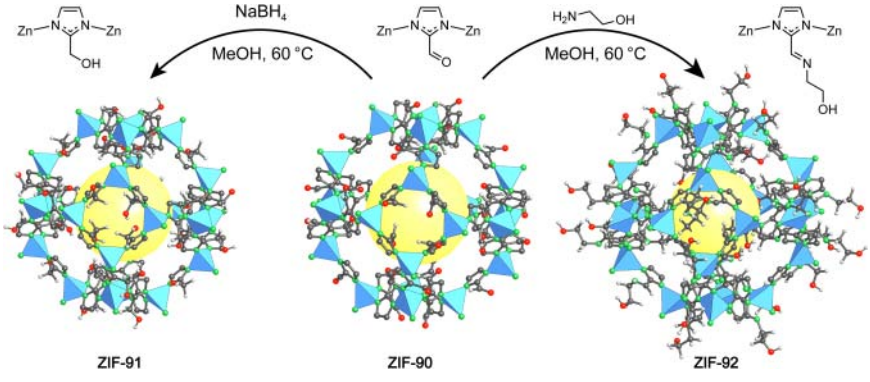

Figure 20.9 Post-synthetic functionalization of ZIF-90. The aIM linker in ZIF-90 (center) can either be reduced to yield alcohols (left, ZIF-91) or reacted with amines to yield the corresponding imines (right, ZIF-92). In both cases, the porosity and crystallinity of the material are retained. Only one cage is shown and all hydrogen atoms on the imidazolate are omitted for clarity. Color code: Zn, blue; C, gray; N, green; O, red.

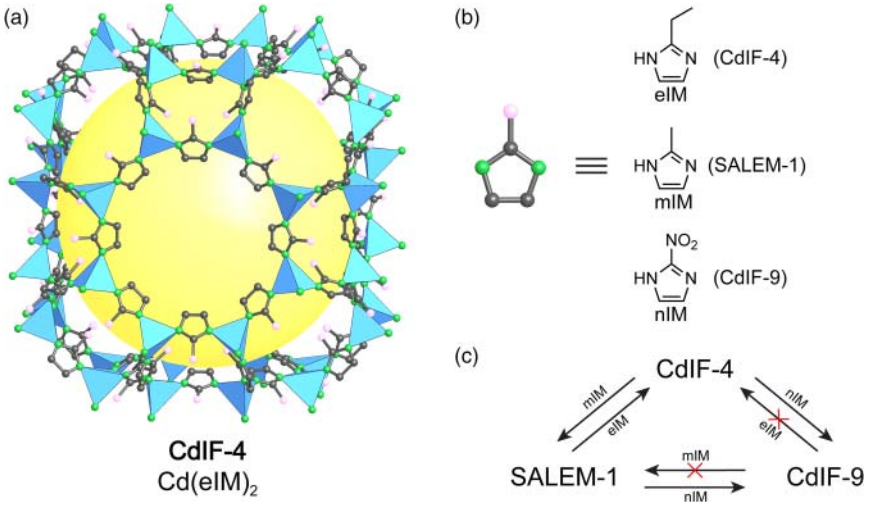

Figure 20.10 Linker exchange reactions in CdIF-4 [32]. (a) The **rho** net of CdIF-4 is built from eIM linkers connecting Cd^{2+} centers. (b) Linker exchange reactions using three differently functionalized imidazole linkers have been studied, yielding three ZIFs in single-crystal to single-crystal transformations. (c) Possible linker exchange reactions between CdIF-4, CdIF-9, and SALEM-1.

Such modifications find use in the preparation of mixed-matrix membranes (MMMs). MMMs are an intensely studied area of ZIF research with focus on applications such as gas separation. Many methods used to prepare MMMs take advantage of PSMs. One example is the deposition of ZIF-90 on an alumina surfaces. This is achieved by modifying an alumina surface with 3-aminopropyltriethoxysilane (APTES) to provide free amines for consecutive imine condensation with the aIM linkers and subsequent *in situ* crystallization of ZIF-90 on the surface [30]. The remaining unmodified aIM linkers can then be functionalized in order to tune the properties of the membranes [31]. ZIFs have also been shown to be good candidates for linker exchange reactions [32]. The 2-ethylimidazole (eIM) linker in CdIF-4, a cadmium-based ZIF with underlying **rho** topology, can be exchanged by nIM or mIM under relatively mild conditions in a single-crystal to single-crystal transformation affording CdIF-9 and SALEM-1, respectively (Figure 20.10). The linker exchange in MMMs is another tool to fine-tune the properties of the membrane as demonstrated for the adjustment of the interplay between selectivity and permeability of ZIF-7 MMMs [33].

20.6 Summary

In this chapter, we introduced ZIFs, a special subclass of MOFs. We saw that similarly to inorganic zeolites, the structures of ZIFs are constructed from tetrahedral nodes connected by linkers. The combination of tetrahedral single-metal nodes and imidazole-based linkers results in tetrahedral structures that feature large cages that are connected through narrow windows. Even though ZIFs are

only composed of linked tetrahedra, the structural diversity seems limitless. We discussed the structural features of ZIFs, general synthetic approaches, and highlighted some frequently encountered topologies. The steric index was introduced as a means to target the formation of ZIFs with large cages and we showed that analogous to MOFs, the organic imidazolate linkers can be functionalized using PSM.

References

1 Cronstedt, A.F. (1756). *Rön och beskrifning om en obekant bärg art, som kallas Zeolites*. Stockholm: Svenska Vetenskaps akademiens Handlingar (trans. J.L. Schlenker and G.H. Kühl. Proceedings of the 9th International Conference on Zeolites. 1993).

2 Damour, A. (1840). Über das Bleigummi und thonerdhaltiges phosphorsaures Bleioxyd von Huelgoat. *Annales des Mines* 17: 191.

3 de St. Claire-Deville, H. (1862). Reproduction de la levyne. *Comptes Rendus* 54 (1862): 324–327.

4 (a) Friedel, G. (1896). New experiments on zeolites. *Bulletin de la Société Française de Minéralogie* 19: 363–390. (b) Friedel, G. (1896). Sur quelques propriétés nouvelles des zéolithes. *Bulletin de la Société Française de Minéralogie, Paris* 19: 94–118.

5 (a) Sherman, J.D. (1999). Synthetic zeolites and other microporous oxide molecular sieves. *Proceedings of the National Academy of Sciences* 96 (7): 3471–3478. (b) Barrer, R.M. (1945). Separation of mixtures using zeolites as molecular sieves. I. Three classes of molecular-sieve zeolite. *Journal of the Society of Chemical Industry* 41 (12): 130–133.

6 (a) Barrer, R.M. (1981). Zeolites and their synthesis. *Zeolites* 1 (3): 130–140. (b) Barrer, R.M. (1948). 33. Synthesis of a zeolitic mineral with chabazite-like sorptive properties. *Journal of the Chemical Society (Resumed)* 127–132.

7 Wilson, S.T., Lok, B.M., Messina, C.A. et al. (1982). Aluminophosphate molecular sieves: a new class of microporous crystalline inorganic solids. *Journal of the American Chemical Society* 104 (4): 1146–1147.

8 Flanigen, E.M., Lok, B.M., Patton, R.L., and Wilson, S.T. (1986). Aluminophosphate molecular sieves and the periodic table. *Pure and Applied Chemistry* 58 (10): 1351–1358.

9 (a) Baerlocher, C., McCusker, L.B., and Olson, D.H. (2007). *Atlas of Zeolite Framework Types*. Elsevier. (b) Corma, A., Díaz-Cabañas, M.J., Jiang, J. et al. (2010). Extra-large pore zeolite (ITQ-40) with the lowest framework density containing double four- and double three-rings. *Proceedings of the National Academy of Sciences of the United States of America* 107 (32): 13997–14002. (c) Flanigen, E.M., Broach, R.W., and Wilson, S.T. (2010). Introduction. S. Kulprathipanja In: *Zeolites in Industrial Separation and Catalysis*, Wiley-VCH 1–26.

10 (a) Eddaoudi, M., Sava, D.F., Eubank, J.F. et al. (2015). Zeolite-like metal-organic frameworks (ZMOFs): design, synthesis, and properties. *Chemical Society Reviews* 44 (1): 228–249. (b) Wang, B., Cote, A.P., Furukawa, H.

et al. (2008). Colossal cages in zeolitic imidazolate frameworks as selective carbon dioxide reservoirs. *Nature* 453 (7192): 207–211. (c) Phan, A., Doonan, C.J., Uribe-Romo, F.J. et al. (2010). Synthesis, structure, and carbon dioxide capture properties of zeolitic imidazolate frameworks. *Accounts of Chemical Research* 43 (1): 58–67.

11 Chen, B., Yang, Z., Zhu, Y., and Xia, Y. (2014). Zeolitic imidazolate framework materials: recent progress in synthesis and applications. *Journal of Materials Chemistry A* 2 (40): 16811–16831.

12 Liu, Y., Kravtsov, V.C., Larsen, R., and Eddaoudi, M. (2006). Molecular building blocks approach to the assembly of zeolite-like metal-organic frameworks (ZMOFs) with extra-large cavities. *Chemical Communications* (14): 1488–1490.

13 Liu, Y., Kravtsov, V.C., and Eddaoudi, M. (2008). Template-directed assembly of zeolite-like metal-organic frameworks (ZMOFs): a usf-ZMOF with an unprecedented zeolite topology. *Angewandte Chemie International Edition* 47 (44): 8446–8449.

14 (a) Férey, G., Mellot-Draznieks, C., Serre, C., and Millange, F. (2005). Crystallized frameworks with giant pores: are there limits to the possible? *Accounts of Chemical Research* 38 (4): 217–225. (b) Férey, G., Mellot-Draznieks, C., Serre, C. et al. (2005). A chromium terephthalate-based solid with unusually large pore volumes and surface area. *Science* 309 (5743): 2040–2042. (c) Férey, G., Serre, C., Mellot-Draznieks, C. et al. (2004). A hybrid solid with giant pores prepared by a combination of targeted chemistry, simulation, and powder diffraction. *Angewandte Chemie International Edition* 116 (46): 6456–6461.

15 Baburin, I., Leoni, S., and Seifert, G. (2008). Enumeration of not-yet-synthesized zeolitic zinc imidazolate MOF networks: a topological and DFT approach. *The Journal of Physical Chemistry B* 112 (31): 9437–9443.

16 Huang, X., Zhang, J., and Chen, X. (2003). $[Zn(bim)_2]\cdot(H_2O)_{1.67}$: a metal-organic open-framework with sodalite topology. *Chinese Science Bulletin* 48 (15): 1531–1534.

17 (a) Huang, X.-C., Lin, Y.-Y., Zhang, J.-P., and Chen, X.-M. (2006). Ligand-directed strategy for zeolite-type metal-organic frameworks: zinc(II) imidazolates with unusual zeolitic topologies. *Angewandte Chemie International Edition* 45 (10): 1557–1559. (b) Banerjee, R., Phan, A., Wang, B. et al. (2008). High-throughput synthesis of zeolitic imidazolate frameworks and application to CO_2 capture. *Science* 319 (5865): 939–943.

18 Yang, J., Zhang, Y.-B., Liu, Q. et al. (2017). Principles of designing extra-large pore openings and cages in zeolitic imidazolate frameworks. *Journal of the American Chemical Society* 139 (18): 6448–6455.

19 Fu, Y.-M., Zhao, Y.-H., Lan, Y.-Q. et al. (2007). A chiral 3D polymer with right- and left-helices based on 2,2′-biimidazole: synthesis, crystal structure and fluorescent property. *Inorganic Chemistry Communications* 10 (6): 720–723.

20 Park, K.S., Ni, Z., Côté, A.P. et al. (2006). Exceptional chemical and thermal stability of zeolitic imidazolate frameworks. *Proceedings of the National Academy of Sciences of the United States of America* 103 (27): 10186–10191.

21 Hayashi, H., Cote, A.P., Furukawa, H. et al. (2007). Zeolite A imidazolate frameworks. *Nature Materials* 6 (7): 501–506.

22 Zhang, J., Wu, T., Zhou, C. et al. (2009). Zeolitic boron imidazolate frameworks. *Angewandte Chemie International Edition* 48 (14): 2542–2545.

23 Chen, W.-T., Fang, X.-N., Luo, Q.-Y. et al. (2007). Poly[μ_2-4,4′-bipyridine-di-μ_2-bromido-cadmium(II)], with novel colour-tunable fluorescence. *Acta Crystallographica Section C: Crystal Structure Communications* 63 (9): 398–400.

24 Masciocchi, N., Bruni, S., Cariati, E. et al. (2001). Extended polymorphism in copper(II) imidazolate polymers: a spectroscopic and XRPD structural study. *Inorganic Chemistry* 40 (23): 5897–5905.

25 Tian, Y.-Q., Cai, C.-X., Ren, X.-M. et al. (2003). The silica-like extended polymorphism of cobalt(II) imidazolate three-dimensional frameworks: X-ray single-crystal structures and magnetic properties. *Chemistry – A European Journal* 9 (22): 5673–5685.

26 Wu, T., Bu, X., Zhang, J., and Feng, P. (2008). New zeolitic imidazolate frameworks: from unprecedented assembly of cubic clusters to ordered cooperative organization of complementary ligands. *Chemistry of Materials* 20 (24): 7377–7382.

27 Spek, A., Duisenberg, A., and Feiters, M. (1983). The structure of the three-dimensional polymer poly [μ-hexakis(2-methylimidazolato-*N*,*N*′)-triiron(II)],$[Fe_3(C_4H_5N_2)_6]_n$. *Acta Crystallographica Section C: Crystal Structure Communications* 39 (9): 1212–1214.

28 Wu, T., Bu, X., Liu, R. et al. (2008). A new zeolitic topology with sixteen-membered ring and multidimensional large pore channels. *Chemistry – A European Journal* 14 (26): 7771–7773.

29 Morris, W., Doonan, C.J., Furukawa, H. et al. (2008). Crystals as molecules: postsynthesis covalent functionalization of zeolitic imidazolate frameworks. *Journal of the American Chemical Society* 130 (38): 12626–12627.

30 (a) Huang, A., Bux, H., Steinbach, F., and Caro, J. (2010). Molecular-sieve membrane with hydrogen permselectivity: ZIF-22 in LTA topology prepared with 3-aminopropyltriethoxysilane as covalent linker. *Angewandte Chemie International Edition* 122 (29): 5078–5081. (b) Huang, A., Dou, W., and Caro, J.r. (2010). Steam-stable zeolitic imidazolate framework ZIF-90 membrane with hydrogen selectivity through covalent functionalization. *Journal of the American Chemical Society* 132 (44): 15562–15564.

31 Huang, A. and Caro, J. (2011). Covalent post-functionalization of zeolitic imidazolate framework ZIF-90 membrane for enhanced hydrogen selectivity. *Angewandte Chemie International Edition* 50 (21): 4979–4982.

32 (a) Karagiaridi, O., Bury, W., Sarjeant, A.A. et al. (2012). Synthesis and characterization of isostructural cadmium zeolitic imidazolate frameworks via solvent-assisted linker exchange. *Chemical Science* 3 (11): 3256–3260.

33 Al-Maythalony, B.A., Alloush, A.M., Faizan, M. et al. (2017). Tuning the interplay between selectivity and permeability of ZIF-7 mixed matrix membranes. *Matrix* 13: 25.